



Published in final edited form as:

J Ocul Pharmacol Ther. 2004 June ; 20(3): 217–236.

Preventive Versus Treatment Effect of Ag3340, a Potent Matrix Metalloproteinase Inhibitor in a Rat Model of Choroidal Neovascularization

MOHAMMED EL BRADEY¹, LINGYUN CHENG¹, DIRK-UWE BARTSCH¹, KRZYSTOF APPELT², NUTTAWUT RODANANT¹, GERMAINE BERGERON-LYNN¹, and WILLIAM R. FREEMAN¹

¹University of California, San Diego, Jacobs Retina Center, and Shiley Eye Center, La Jolla, CA

²Agouron Pfizer, La Jolla, CA

Abstract

Purpose: AG3340 (prinomastat) is a nonpeptidic, small-molecular-weight, synthetic matrix metalloproteinase inhibitor (MMPI) with selective inhibitory action of MMP-2, MMP-9, MMP-3, and MT-MMP1. We evaluated AG3340 injected intravitreally to treat choroidal neovascularization in a laser induced rat CNV model. **Methods:** In the pretreatment group, the drug was injected the same day after induction of choroidal neovascularization by diode laser. In the treatment group, the drug was injected 2 weeks after induction of choroidal neovascularization (CNV). Fluorescein and indocyanine green angiography were performed to evaluate CNV. ERG recordings and histology were performed to assess toxicity and the CNV lesions. **Results:** When used at the time of CNV induction, 62.8% of lesions in control versus 22.8% of the laser lesions in treated eyes developed CNV ($p < 0.0001$). The invading fibrovascular complex was thicker in the control eyes than that in the treated eyes. No signs of toxicity were detected. When used to treat established CNV, the percentage of leakage in treated and control eyes were 54.1% and 58.9% respectively ($p > 0.05$). Prinomastat was effective when given at the time of induction of CNV in the rat model. Administration of prinomastat 2 weeks after laser induction did not show efficacy. **Conclusion:** Prinomastat was active in the earliest stages of experimental CNV. It might be best used in combination with photodynamic therapy to inhibit recurrence of CNV from temporarily closed new vessels.

INTRODUCTION

Age-related macular degeneration associated choroidal neovascularization (CNV) is the major cause of severe visual loss in patients with age-related macular degeneration (1). The newly formed vessels originate from the choroid and enter the subretinal space, where they are recognized clinically by fluorescein angiography leakage during angiography. The blood vessels leak fluid beneath the retina, causing reversible visual loss followed by bleeding and scarring that result in permanent loss of central vision (2).

No highly effective treatment of CNV has yet been developed. Laser photocoagulation has long been used as a treatment modality for CNV. However, this treatment often produces damage to the sensory retina, incomplete CNV closure, and frequent recurrence resulting in visual loss (3). A more recent option of at least modest benefit in cases of subretinal CNV is

Correspondence to: WILLIAM R. FREEMAN.

Reprint Requests: William R. Freeman University of California, San Diego Jacobs Retina Center 9415 Campus Point Drive La Jolla, CA 92093-0946 E-mail: freeman@eyecenter.ucsd.edu.

photodynamic therapy. However, it is expensive and studies show that benefit is limited to eyes with classical patterns of CNV, which represent a minority of cases (4). Radiation therapy for CNV has a less favorable outcome with considerable side-effects (5). Submacular surgery for removal of CNV has a disappointing result in type I membrane (Sub RPE type), which is typical of age related macular degeneration (6). Macular translocation surgery for CNV is still evolving with variable results and of high-risk complications (5).

Current surgical treatment modalities are designed to destroy or remove the abnormal blood vessels and do not address the underlying pathologic changes and stimuli responsible for neovascularization. Therefore, recurrent neovascularization and permanent visual loss occur in the majority of patients who initially have had successful treatment (7).

Pharmacologic therapy with antiangiogenic drugs is a theoretical alternative for the treatment of CNV. This type of therapy may permit CNV treatment without destruction of the overlying retina. It also may prevent recurrence following laser treatment and possibly be used as a prophylaxis (8). There are a variety of candidate drugs under consideration including matrix metalloproteinase inhibitors, VEGF inhibitors, TNP-470, interferon alpha, indomethacin, tranilast, kinase inhibitors, thalidomide, and others (8-16).

Choroidal neovascularization shares many of the same pathologic steps with other forms of angiogenesis. The process is initiated by the release of angiogenic factors, which stimulate the endothelial cells to secrete proteolytic enzymes (matrix metalloproteinase enzymes). These proteolytic enzymes release the endothelial cells from their basement membrane and also degrade the extracellular matrix surrounding the blood vessels facilitating endothelial-cell migration. The majority of endothelial cells proliferate and form vascular loops, which are ultimately canalized to establish blood flow (17-18). It is clear that, whatever the stimuli, the process of proteolysis by MMPs is an important step in the final common pathway of angiogenesis. Therefore, inhibition of the process of CNV at this level may be an attractive field of research rather than targeting the inciting stimuli themselves, which include many cytokines and other factors (19). Indeed it has recently been shown that there is reduced CNV in MMP-9 deficient mice (20).

AG3340 was developed by using X-ray crystallographic techniques (21). AG3340 is a nonpeptidic, small-molecular-weight, synthetic matrix metalloproteinase inhibitor (MMPI), as shown in Figure 1, with selective inhibitory action of MMP-2, MMP-3, MMP-9, and MTMMP-1 (22). This drug was first used in human clinical trials for the treatment of advanced prostate and lung cancer. The drug inhibits tumor growth, invasion, and metastasis via an antiangiogenic effect. The drug also inhibits the basement-membrane destruction that accompanies cancer invasion (23).

In this study, we evaluated the efficacy and toxicity of AG3340 injected intravitreally as a preventive and treatment modality in a rat model of CNV.

MATERIALS AND METHODS

This experiment was carried out on 66 female Brown Norway rats (Harlan Sprague-Dawley Inc, Indianapolis, IN) weighting between 180 and 220 g. All procedures were performed with strict adherence to guidelines for animal care and experimentation prepared by the Association for Research in Vision and Ophthalmology. Choroidal neovascularization was induced in 60 rats bilaterally. The other 6 rats (12 eyes) had no experimental procedure and were only used as a normal control for histologic sections and toxicity study. The rats with induced CNV were randomly divided into two groups; group A (pretreatment group), which included 35 rats and group B (treatment group), which included 25 rats.

Induction of Choroidal Neovascularization

Anesthesia was induced by intramuscular injection of a mixture of 56 mg/kg of ketamine and 6 mg/kg of xylazine. Then, the pupil was dilated by topical application of a combination of tropicamide 1% and phenylephrine hydrochloride 2.5%. Eight laser lesions were applied in each eye between large blood vessels 2–4-disc diameters from the optic nerve using diode laser photocoagulator (Oculight Slx; Iris Medical, Mountain View, CA). Ocular rat contact lens (Ocular Instruments Inc., Bellevue, WA) filled with 1 drop of methylcellulose was applied to the rat cornea. The selected laser parameters were as follows: 810 nanometer wavelength, 0.1 second duration, 200 milliwatts power and 75 μ m spot size. The laser-aiming beam was focused on Bruch's membrane. The aim was to rupture Bruch's membrane so the choroidal blood vessel would invade the subretinal space forming choroidal neovascularization. The sure sign of Bruch's membrane rupture by laser was the formation of bubbling at the site of laser application with or without hemorrhage. Each laser spot was given a number between 1 and 8 according to its relation to the optic nerve as follows: 1, superior to the optic nerve; 2, upper anterior; 3, anterior; 4, lower anterior; 5, lower; 6, lower posterior; 7, posterior; and 8, upper posterior.

All laser application lesions were numbered according to their position in this manner. The pattern was arranged so that lesion numbers 2, 3, and 4 were on one vertical line anterior to the optic nerve. Lesion numbers 1 and 5 were on the same line coincident with the optic nerve. Spot numbers 6, 7, and 8 were on the same vertical line posterior to the optic nerve. These locations of the laser lesions were chosen so that lesion numbers 2, 3, and 4 were together in one histologic section. In addition, lesions 1, 5, and the optic nerve were in one histologic section. Finally, lesions numbers 6, 7, and 8 were in one histologic section.

Drug Injection

In group A (pretreatment group), the drug was injected the same day after induction of choroidal neovascularization by diode laser. In group B (treatment group), the drug was injected 2 weeks after induction of choroidal neovascularization and just after acquiring the first set of fluorescein angiography to study the effect of the drug on the already established choroidal neovascularization. A sterile suspension of 0.07 mg AG3340-HA (Agouron Pharmaceuticals, Inc., La Jolla, CA) in 7 μ L of the vehicle (sodium hyaluronate) was injected in the right eyes while the left eyes of the all 60 rats received sterile 7 μ L of the vehicle using a sterile 50 μ L Hamilton syringe (Hamilton Co., Reno, NV) attached to a 30G needle and under visualization using an Olympus dissecting microscope (model SZH, Olympus Industrial America Inc., Nanuet, NY). The dose and the technique of drug injection was the same in both the pretreatment and treatment groups and the only difference was the timing of drug injection.

Clinical Evaluation

All rats were examined on day 1, day 3, day 5, and then weekly after drug injection up to the time of sacrifice. It was determined that the animals were able to eat and behave normally after the laser treatments. The examination was performed by slit lamp to evaluate the anterior segment and by indirect ophthalmoscopy using a 40-diopter lens to evaluate the retina and vitreous. All relevant ophthalmic and systemic findings were recorded and the rate of disappearance of drug aggregates from the vitreous was also evaluated.

Fluorescein Angiography

Pretreatment group—Fluorescein angiography was performed in all 35 rats 2 and 4 weeks after simultaneous laser induction of CNV and drug injection. After 4 weeks, 17 rats were sacrificed and their eyes were processed for histologic studies. Another set of fluorescein angiographies was acquired in the remaining 18 rats at 8 weeks. Subsequently, 9 of these 18 rats were sacrificed and their eyes were processed for histologic studies. The last set of

fluorescein angiographies was performed on the remaining 9 rats at 12 weeks. The rats were then sacrificed and their eyes processed for histology.

Treatment group—Fluorescein angiography was performed in all 25 rats at 2 and 4 weeks after induction of CNV by laser. After 4 weeks, 13 rats were sacrificed and their eyes processed for histologic studies. Another set of fluorescein angiograms were acquired in the remaining 12 rats at 8 weeks. Subsequently, 6 of these 12 rats were sacrificed and their eyes were processed for histologic studies. The last set of fluorescein angiograms was done to the remaining 6 rats at 12 weeks. The rats were then sacrificed and their eyes processed for histologic studies.

Technique of Fluorescein Angiography—We used a confocal scanning laser ophthalmoscope with two laser sources to illuminate the retina (Heidelberg Retina Angiography, Heidelberg Engineering, Carlsbad, CA). The instrument uses two lasers with three wavelengths as a light source for scanning fundus illumination: The argon laser provided two wavelengths, 488 nm and 514 nm. A 514-nm laser was used to provide red-free photographs while 488-nm blue-light was used for excitation during fluorescein angiography. The second laser was a diode laser (795 nm) that provided illumination, which fluoresces at 835 nm.

After anesthesia and pupillary dilation, 0.1 mL of a 25% sodium fluorescein (Alcon, Fort Worth, TX) was injected into the rat-tail vein, using a 28.5 G insulin syringe, and fluorescein photos were simultaneously recorded in digital format. After injection, the camera alternated between both eyes taking images for 10 minutes. The camera software allowed us to prepare a digital version of a composite fundus image from the already taken images and allowed us to visualize the entire fundus, including all the performed laser lesions in one image.

Evaluation of Laser Lesions by Fluorescein Angiography—For fluorescein angiography evaluation, each laser spot was evaluated as follows:

- *Leaking spot*—The spot demonstrated an increase in size of hyperfluorescence over time.
- *Nonleaking spot*—The spot revealed only staining without an increase in size of hyperfluorescence.
- *Nonevaluatable spot*—If the fluorescein angiography could not evaluate the spot due to masking by the overlying hemorrhage, the spot was considered to be nonevaluatable.

ERG Methods

Subjects and time points—ERG recordings and histology were performed bilaterally on 8 of 9 rats that were kept for 12 weeks in the pretreatment group. The ninth rat was excluded from the ERG study due to inability to record the ERG due to technical difficulties. ERG was performed at 4 time points: the first one was before laser induction of CNV (before any experimental procedure); the second one was 4 weeks later; the third one was 8 weeks later; and the last one was 12 weeks later just before sacrifice and 1 day after the last set of fluorescein angiograms.

ERG Procedure

After pupillary dilation, the rats were left for dark adaptation in a completely dark room for 45 minutes. Then, a dim red light was used to complete the procedure. The rats were anesthetized by intramuscular injection of ketamine 21 mg/kg and xylazine 5.5 mg/kg. Corneas were treated further with proparacaine hydrochloride (Ophthaine, Apoticon, Princeton, NJ). Each rat was

placed on a movable platform in a prone position. The electrodes were applied as follows: two gold-loop electrodes were applied on the cornea one for each eye. Two subdermal needle reference electrodes were applied, one to each cheek. Another two clip electrodes were applied one for each ear, serving as ground electrodes. All stimuli were presented in the Ganzfeld stimulator and controlled by a control station as described previously (24). All stimuli came from photo stimulator, (Model PS22, Grass instrument company, Quincy, MA). The flash was positioned 25 cm above the rat's head to deliver white light flashes, which were reflected from the inner high reflectance coating of the Ganzfeld dome to the rat eye. The photo stimulator flash switch was set at single flash position and the flash intensity was set at 1 (no neutral density filters were used), and the luminance on the surface of the eye was approximately 2.8 Lux at intensity 1. The duration of each stimulus was 10 microseconds. The inter stimulus interval was 30 seconds. Five fixed power stimuli were performed for each eye at each time point. The five responses from each eye were collected and amplified by a regulated power supply model RPS 21 and a high performance AC amplifier (model P 511, Grass instrument division, West Warwick, RI). Low- and high-frequency cutoffs were set at 1.0 and 1000 Hz. Amplification was set to be 5000. Amplified signals were digitalized through an A/D (analog to digital) converter (model PCI-1200; National Instruments, Austin, TX) and the data were saved in a personal computer. Electroretinograms (ERGs) elicited by five stimuli were averaged using custom software (I- System Data Acquisition software, Los Angeles, CA). All measurements of a and b wave amplitudes and implicit times were done digitally using the software program. The mean values of these data for both eyes in the 8 rats were compared at each time point using Student's *t*-test.

Rat Sacrifice

There were three time points for rat sacrifice as follows:

- *First time point (4 weeks)*—17 rats of the pretreatment group and 13 from the treatment group were sacrificed at week 4, one day after performance of fluorescein angiography. Another 2 rats of the same gender, species, and age that did not have any procedures done, were also sacrificed to serve as normal histologic controls.
- *Second time point (8 weeks)*—Another 9 rats of the pretreatment group and 6 rats from the treatment group were sacrificed at week 8, one day after performance of fluorescein angiography. Another 2 rats of the same gender, species, and age that did not have any procedures done were also sacrificed to serve as normal histologic controls. This time point was selected to evaluate the healing pattern after laser in both treated and control eyes.
- *Third time point (12 weeks)*—The last 9 rats of the pretreatment group were sacrificed at week 12, 1 day after performance of fluorescein angiography and just after performance of the last ERG. The last 6 rats of the treated group were also sacrificed at this time point. Another 2 rats of the same gender, species, and age that did not have any procedures done were also sacrificed to serve as normal histologic controls. This time point was chosen to detect any histologic evidence of late drug toxicity in the treated eyes.

The order of rat sacrifices was performed randomly according to their labeled numbers and none of the rats were selected to be sacrificed at any time point.

All rats were sacrificed using *in vivo* perfusion fix technique using a mixture of 2.5% gluteraldehyde and 2% paraformaldehyde. The eyes were then enucleated and histologic sections were prepared for both light microscopy and electron microscopic evaluation.

Statistical analysis

All the statistical analysis was performed using JMP software version 5.02 (SAS Inc., Carey, NC).

RESULTS

Results of the Pretreatment Study

This study was carried out on 35 Brown Norway rats to study the efficacy and toxicity of AG3340 as a prophylactic treatment of choroidal neovascularization. Diode laser photocoagulation was used to induce CNV bilaterally in 35 rats. The basic characteristics of the laser lesions were studied and documented by color fundus photos in both treated and control eyes (Figs. 2 and 3).

As illustrated in Table 1, the differences between the control and treatment groups in baseline characteristics of laser lesions was statistically insignificant.

Table 2 illustrates the percentage of leakage in treated and control eyes at different time points as seen by the use of the scanning laser ophthalmoscope. At the 4-week time point, 62.8% of the laser lesions in the control eyes were leaking indicating the formation of CNV while only 22.8% were leaking in the treated eyes. The difference was statistically significant ($p < 0.0001$).

Leakage reached its maximum at 4 weeks in both treated and control animals. For this reason, a 4-week time point was chosen to be the primary time of evaluation.

The drug prevented the formation of choroidal neovascularization completely in 5 eyes (14.3%) and 13 eyes of the treated group developed only one leaking laser spot. Thus, 18 of 35 eyes (51.4%) of the treated eyes either had one or no leaking laser lesions. On the other hand, all the control eyes had more than one leaking laser spot (Fig. 4).

Seventeen eyes (48.6%) of the control group had more than 4 leaking lesions while none of the treated eyes had more than 4 leaking lesions. In the treated group, the mean number of leaking lesions per eye was $1.49 \text{ spot} \pm 0.92$ versus $4.43 \text{ spot} \pm 1.357$ in the controls.

CNV lesions associated with hemorrhage at the time of laser were strongly associated with the increased formation of choroidal neovascularization in both control and treated eyes. As shown in Table 3, 43% of laser lesions associated with bubbling in control eyes developed CNV versus 79.4% of laser lesions associated with hemorrhage developed CNV. The difference was statistically significant ($p < 0.0001$).

Although the number of leaking lesions was much lower in treated than in the control eyes, the leakage in treated eyes was also more in lesions associated with hemorrhage than in lesions associated only with bubbling. 13.2% of laser lesions associated with bubbling developed CNV versus 31.1% of laser lesions associated with hemorrhage. The difference was statistically significant ($p = 0.0008$).

Even in the eyes that had hemorrhagic laser lesions, the drug had an inhibitory effect on the development of CNV. The difference in the percentage of leakage in lesions associated with hemorrhage in both groups at the 4-week time point was statistically significant ($p < 0.0001$ chi-square test).

The distribution of the leaking laser lesions according to their locations in the retina was also evaluated. Chi-square testing revealed no significant preference of the leaking lesions to certain retinal locations, with nearly even distribution in both treated eyes ($p = 0.4$) and controls ($p = 0.44$). In treated eyes, the percentages of leakage of upper versus lower and anterior versus

posterior laser lesions were compared. The difference was statistically insignificant, indicating an even distribution of the inhibitory effect of the drug.

With regard to the ERG data there was no significant difference in the ERG data between the treated and control groups at all time points up to 3-month follow up (Figs. 5 and 6).

Ophthalmoscopic and Slit-Lamp Evaluation Results

All the rats were examined using a slit lamp and indirect ophthalmoscopy on days 1, 3, 5, and 7 after drug injection and weekly thereafter until time of sacrifice.

Drug aggregates

Following the intravitreal drug injection, small aggregates of white drug aggregates were clinically observed in the vitreous at the injection site (Fig. 7). The density of these aggregates decreased over the next 72 hours. At 5 days, few drug aggregates were still present and disappeared by day 7 postinjection.

Anterior segment evaluation

None of the treated or control eyes developed any signs of anterior segment complications. The cornea and lens remained clear at all times of follow-up. No signs of uveitis were detected during the follow-up period. The intraocular pressure was not evaluated in this experiment.

Posterior segment evaluation

The vitreous The vitreous was clear during the follow-up period in both treated and control eyes except for the drug aggregates, which localized at the site of injection.

Laser lesions Fundus examination of the laser lesions immediately after photocoagulation revealed the presence of an air bubble under the retina, which was localized to the area of laser burn. The bubbles then shrank within minutes and the overlying retina became edematous (Figs. 2 and 3). In the lesions associated with hemorrhage, the bubbles were masked by blood. The blood overlying some laser lesions showed gradual absorption by time. However the rate of blood clearance was variable according to the blood density at the time of laser applications. Interestingly, there was no clinically observable difference between leaking and nonleaking lesions. For this reason the main method of evaluation of the laser lesions was by fluorescein angiography. Also no clinical differences were detected between the laser scars formed in both treated and control eyes. The retina in between laser lesions was clinically normal in both groups.

Histological Results

Four-week time point—All of the lesions in both treated and control eyes demonstrated disruption of the Bruch's membrane with degeneration of the overlying RPE cells, photoreceptors, outer nuclear layer, and outer plexiform layer as well as partial disruption of the inner nuclear layer. In some lesions, the degree of damage to the retina extended internally up to the ganglion cell layer.

Lesions that demonstrated leakage on fluorescein angiography in both control and treatment groups revealed the presence of a newly formed fibrovascular complex tissue in the subretinal space. This fibrovascular complex was noted to proliferate and extended much more beyond the area of the break in Bruch's membrane. This fibrovascular complex was formed from collagen fibers, fibroblasts, and proliferating endothelial cells forming new blood vessels, some of which had red blood cells (RBCs) in their lumen. RPE cells were found at the edge of this neovascular complex (Fig. 8).

There were two major histologic differences in the leaking lesions between treated and control eyes; first, the invading fibrovascular complex was much thicker in the control eyes, second, the proliferating endothelial cells were much more prevalent in the control eyes with a tendency to form large new blood vessels containing RBCs. In treated eyes, the number of endothelial cells was much fewer, and the lumen of blood vessels was small, lacking RBCs in the lumen (Figs. 9 and 10).

The nonleaking lesions in both groups were essentially fibrotic. However, the thickness of these fibrous scars was greater in control eyes. Interestingly, scattered endothelial cells were also detected in some sections of these nonleaking lesions in both groups but no RBCs were detected in their lumens.

Another two types of cells were detected in leaking and nonleaking lesions: macrophages and pigment-laden cells. These cells were scattered in the choroid underneath the lesion, in the fibrovascular complex, in the overlying degenerated retina, and in the nearby retinal layers. There were no differences in the density and distribution of these cells in both treated eyes and controls (Fig. 11).

The area of the retina between laser lesions in treated eyes was also examined histologically by both light and electron microscopy. The periphery of the retina was studied in histologic sections, especially the area near the drug injection and the area underneath the drug aggregates. No toxic changes were detected in any treated eyes as compared to the retina of normal rats of same age group (i.e., the four eyes of two rats that did not undergo any procedure and kept for 4 weeks to serve as a histology controls). The retina in these areas was of normal thickness; all retinal layers were demonstrated clearly; and no inflammatory cells were detected in the choroid, retina, or overlying vitreous. Histologic sections of cornea, iris, and ciliary body were also normal without any signs of drug toxicity.

The lesions showed similar histological characteristics to what was described at the 4-week time point. However, the major difference was in the RPE healing pattern in both treated and controls. In treated eyes, the RPE proliferated to form a monolayer of RPE overlying the fibrovascular complex. The RPE cells at the edge of the scar also formed one layer. However in control eyes, the RPE showed marked proliferation with healing in multiple irregular layers. The RPE cells at the edge of the scar were formed of many layers (Fig. 12).

In treated eyes, the retina between laser lesions and at the retinal periphery near the site of injection was normal as compared to the normal control rats of the same age group (i.e., the 4 eyes of 2 rats that did not undergo any procedure and kept for 8 weeks to serve as histology controls).

12-Week Time Point—No signs of late toxicity were detected in either the retina nor optic nerve compared to the normal eyes of the same age at this time point (i.e., the 4 eyes of the two rats that did not undergo any procedure and were kept for 12 weeks to serve as histology controls). The sections were evaluated by both light and electron microscope.

Results of the Treatment Study

This study was carried out on 25 Brown Norway rats to study the efficacy of AG3340 as a treatment modality of already formed CNV. Diode laser photocoagulation was used to induce CNV bilaterally in 25 rats. As shown in Table 4 the drug proved to have minimal effect in the treatment of established CNV. At 4 weeks time (2 weeks postinjection), the percentage of leakage in treated and control eyes was 54.1% and 58.9%, respectively. The difference was statistically insignificant. A similar insignificant effect was observed at the 8- and 12-week time point.

DISCUSSION

Increased expression of matrix metalloproteinase-2 (MMP-2) activity has been detected in eyes with choroidal neovascularization as well as in tumors (9,25-31). It has been hypothesized that antiangiogenic therapy would be effective in diseases such as choroidal neovascularization in which angiogenesis is a key component to the pathophysiology (12,25). Prinomastat (AG3340) is a selective inhibitor of MMP-2, 9,13, and membrane-type MMP-1 (MMP-14) enzymes. It has a broad spectrum of antitumor activity in tumor models after oral and intraperitoneal dosing. Preclinical *in vivo* models show that the antitumor activity of prinomastat has been associated with an increased incidence of apoptosis and necrosis of tumor cells and inhibition of cellular proliferation and angiogenesis (26). The MMPs that are inhibited by prinomastat are involved in choroidal neovascularization and, for this reason, we hypothesized that inhibition of these enzymes would have a beneficial effect in an animal model of choroidal neovascularization.

Laser induced CNV is an accepted model of human CNV however it has several differences. The natural history of laser induced CNV is for regression of the neovascularization within 1–2 months of induction. In contrast, human choroidal neovascularization is a more chronic disease. In particular, occult choroidal neovascularization continues to leak and exude over a period of 1–2 years (3-4).

Many investigators have studied antiangiogenic compounds in the rat or monkey model of choroidal neovascularization and have typically used the laser induced CNV model (12, 32-33). To do this, CNV is induced by a high intensity small laser spot directed to the Bruch's membrane area. Typically bubbling is seen, which is taken as evidence of rupture of Bruch's membrane, and such a rupture may be accompanied by hemorrhage. Over the ensuing week, choroidal neovascularization develops.

In order to determine the efficacy of drug therapy on choroidal neovascularization, treatment with the drug can begin prior to the induction of CNV, at the time of induction, or after the induction of CNV. We have reported that “pretreatment” of infectious retinitis due to *Herpes simplex* virus (HSV) is more effective than treating established retinitis, probably because of the fulminant nature of established HSV retinitis (24-34). Similar considerations may apply to laser-induced choroidal neovascularization and, for this reason, we tested the MMP inhibitor prinomastat both in a prophylactic sense (given at the time of laser induction) as well as in the treatment of established CNV.

Our results show that prinomastat is active when given at the time of induction of CNV in the rat model. This is essentially a pretreatment model because the CNV is not present at the time of laser induction (which is also the time that the drug was first used). Two (2) and 4 weeks after laser induction of CNV the amount of CNV leakage was reduced by nearly threefold in Prinomastat-treated animals in this model. These effects were highly significant.

Interestingly, administration of prinomastat 2 weeks after laser induction did not show efficacy. It is important to note that, at this time point, the CNV is maximal in this model. When these animals were followed up to 12 weeks (10 weeks after drug treatment), no difference in CNV was noted between treated and untreated animals.

Based on our studies and others, a clinical trial was performed using prinomastat, given systemically to treat patients with CNV. That trial showed safety but did not show evidence of efficacy. Unfortunately, in humans, prinomastat does have adverse effects, which does limit the maximal dose that could be administered to patients. Nevertheless, it appears that one must be careful when extrapolating results of treatment of CNV in the laser-induced model to CNV in patients. Ongoing clinical studies of an aptamer to VEGF have shown an 80% efficacy in a rodent ROP model and efficacies between 65% and 76% in corneal angiogenesis and human

tumor engraft assays of angiogenesis. Studies of recombinant humanized anti-VEGF antibodies have shown a 75% efficacy in the treatment of established CNV and a higher (92%) efficacy in a prevention study in the same model. Our work shows that one must take into account the different natural histories of the CNV in the human and laser-induced animal models and must also take into consideration the stage of CNV that one is treating. Compounds, such as Prinomastat, which are active in the earliest stages of experimental CNV, might be best used in combination with photodynamic therapy that has an immediate (although temporary) effect on CNV.

REFERENCES

1. Cui JZ, Kimura H, Spee C, Thumann G, Hinton DR, Ryan SJ. Natural history of choroidal neovascularization induced by vascular endothelial growth factor in the primate. *Graefes Arch. Clin. Exp. Ophthalmol* 2000;238:326–333. [PubMed: 10853932]
2. Teeters VW, Bird AC. The development of neovascularization of senile disciform macular degeneration. *Am. J. Ophthalmol* 1973;76:1–18. [PubMed: 4717340]
3. Macular Photocoagulation Study Group. Laser photocoagulation of subfoveal neovascular lesions of age related macular degeneration: Updated findings from two clinical trials. *Arch. Ophthalmol* 1993;111:1200–1209. [PubMed: 7689827]
4. Treatment of Age-Related Macular Degeneration with Photodynamic Therapy (TAP) Study Group. Treatment of age-related macular degeneration with photodynamic therapy neovascularization in age-related macular degeneration with verteporfin: One-year results of 2 randomized clinical trials—TAP report 1. *Arch. Ophthalmol* 1999;117:1329–1345. [PubMed: 10532441]
5. Stokkermans TJ. Treatment of age related macular degeneration. *Clin. Eye Vis* 2000;12:15–35.
6. Grossinklaus HE, Gass JDM. Clinicopathologic correlations of surgically excised type 1 and type 2 submacular choroidal neovascular membranes. *Am. J. Ophthalmol* 1998;126:59–69. [PubMed: 9683150]
7. Seo MS, Kwak N, Ozaki H, et al. Dramatic inhibition of retinal and choroidal neovascularization by oral administration of kinase inhibitors. *Am. J. Pathol* 1999;154:1743–1753. [PubMed: 10362799]
8. Pharmacological Therapy for Macular Degeneration Study Group. Interferon alpha-2a is ineffective for patients with choroidal neovascularization secondary to age related macular degeneration. *Arch. Ophthalmol* 1997;115:865–872. [PubMed: 9230826]
9. Blodi BA, AG3340 Study Group. Effects of prinomastat (AG3340), an angiogenesis inhibitor, in patients with subfoveal choroidal neovascularization associated with age related macular degeneration. *Invest. Ophthalmol. Vis. Sci* 2001;42(suppl):S311.
10. Schwartz SD, Blumenkranz M, Rosenfeld PJ, et al. Safety of rhuFab V2, an anti-VEGF antibody fragment, as a single intravitreal injection in subjects with neovascular age-related macular degeneration. *Invest. Ophthalmol. Vis. Sci* 2001;42(suppl):S522.
11. Guyer DR, Martin DM, Klein M, Haller J. Anti-VEGF therapy in patients with exudative age related macular degeneration. *Invest. Ophthalmol. Vis. Sci* 2001;42(suppl):S522.
12. Ishida A, Kinoshita H, Kobayashi S, Sakabe T. Inhibitory effect of TNP-470 on experimental choroidal neovascularization in a rat model. *Invest. Ophthalmol. Vis. Sci* 1999;40:1512–1519. [PubMed: 10359334]
13. Sakamoto T, Soriano D, Nassarallah J, et al. Effects of intravitreal administration of indomethacin on experimental subretinal neovascularization in subhuman primate. *Arch. Ophthalmol* 1995;113:222–226.
14. Takehana Y, Kurokavva T, Tsukahara Y, Alkahane S, Kitazawa M, Yoshimura N. Suppression of laser induced choroidal neovascularization by oral tranilast in the rat. *Invest. Ophthalmol. Vis. Sci* 1999;40:459–466. [PubMed: 9950606]
15. Ciula TA, Criswell MH, Danis RP, Hill TE. Intravitreal triamcinolone acetate inhibits choroidal neovascularization in a laser-treated rat model. *Arch. Ophthalmol* 2001;119:399–404. [PubMed: 11231773]
16. Ip M, Gorin MB. Recurrence of a choroidal neovascular membrane in a patient with punctate inner choroidopathy treated with daily dose of thalidomide. *Am. J. Ophthalmol* 1996;122:594–595. [PubMed: 8862067]

17. Gass JDM. Pathogenesis of disciform detachment of the neuroepithelium, III: Senile disciform macular degeneration. *Am. J. Ophthalmol* 1967;63:617–644.
18. Casey R, Li W. Factors controlling ocular angiogenesis. *Am. J. Ophthalmol* 1997;124:521–529.
19. Stehi CS, Bailey TA, Luthert PJ, Chong NHV. Matrix metalloproteinase biology applied to vitreoretinal disorders. *Br. J. Ophthalmol* 2000;84:654–666. [PubMed: 10837397]
20. Lambert V, Munaut C, Jost M, Noel A, Werb Z, Foidart J-M, Rakic J-M. Matrix Metalloproteinase-9 contributes to choroidal neovascularization. *Am. J. Pathol* 2002;161:1247–1253. [PubMed: 12368198]
21. Santos O, McDermott CD, Daniels RG, Appelt K. Rodent pharmacokinetics and antitumor efficacy studies with a series of synthetic inhibitors of matrix metalloproteinases. *Clin. Exp. Metastasis* 1997;15:499–508. [PubMed: 9247252]
22. Scantena R. Prinomastat, a hydroxamate-based matrix metalloproteinase inhibitor: A novel pharmacological approach for tissue remodeling-related diseases. *Exp. Opin. Invest. Drugs* 2000;9:2159–2165.
23. Werb Z, Vu TH, Rinkenberger JL, Coussens LM. Matrix degrading proteases and angiogenesis during development and tumor formation [review]. *Acta. Pathol. Microbiol. Immun. Scand* 1999;107:11–8.
24. Cheng L, Hostetler KL, Chaidhawangul S, et al. Treatment or prevention of *Herpes simplex* virus retinitis with intravitreally injected crystalline 1-*O*-hexadecylpropendiol-3-phosphoganciclovir. *Invest. Ophthalmol. Vis. Sci* 2002;43:515–521. [PubMed: 11818399]
25. Garcia RC, Rivero ME, Hagedorn M, McDermott C, Bergeron-Lynn G, Appelt K, Freeman WR. Efficacy of prinomastat (AG3340), a matrix metalloproteinase inhibitor in treatment of retinal Neovascularization. *Curr. Eye Res* 2002;24(1):33–38. [PubMed: 12187492]
26. Ozerdem U, Mach-Hofacre B, Varki N, Folberg R, Mueller AJ, Ochabski R, Pham T, Appelt K, Freeman WR. The Effect of prinomastat (AG3340), a synthetic inhibitor of matrix metalloproteinases, on uveal melanoma rabbit Model. *Curr. Eye Res* 2002;24:86–91. [PubMed: 12187478]
27. Shalinsky DR, Brekken J, Zou H, et al. Broad antitumor and antiangiogenic activities of AG3340, a potent and selective MMP inhibitor undergoing advanced oncology clinical trials. *Ann. N.Y. Acad. Sci* 1999;878:236–70. [PubMed: 10415735]
28. Drummond AH, Beckett P, Brown PD, et al. Preclinical and clinical studies of MMP inhibitors in cancer. *Ann. N.Y. Acad. Sci* 1999;878:228–35. [PubMed: 10415734]
29. Berglin L, Sarman S, van der Ploeg I, Steen B, Ming Y, Itohara S, Seregard S, Kvanta A. Reduced choroidal neovascular membrane formation in matrix metalloproteinase-2-deficient mice. *Invest. Ophthalmol. Vis. Sci* 2003;44:403–408. [PubMed: 12506102]
30. Hoffmann S, Friedrichs U, Eichler W, Rosenthal A, Wiedemann P. Advanced glycation end products induce choroidal endothelial cell proliferation, matrix metalloproteinase-2 and VEGF upregulation *in vitro*. *Graefes Arch. Clin. Exp. Ophthalmol* 2002;240:996–1002. [PubMed: 12483322]
31. Kvanta A, Shen WY, Sarman S, Seregard S, Steen B, Rakoczy E. Matrix metalloproteinase (MMP) expression in experimental choroidal neovascularization. *Curr. Eye Res* 2000;21(3):684–690. [PubMed: 11120556]
32. Eye-Tech Study Group. Preclinical and phase 1A clinical evaluation of an anti-VEGF pegylated aptamer (EYE001) for the treatment of exudative age-related macular degeneration. *Retina* 2002;22(2):143–152. [PubMed: 11927845]
33. Krzystolik MG, Afshari MA, Adamis AP, Gaudreault J, Gragoudas ES, Michaud NA, Li W, Connolly E, O'Neill CA, Miller JW. Prevention of experimental choroidal neovascularization with intravitreal anti-vascular endothelial growth factor antibody fragment. *Arch. Ophthalmol* 2002;120(3):338–346. [PubMed: 11879138]
34. Cheng L, Hostetler KY, Chaidhawangul S, Gardener MF, Ozerdem U, Bergeron-Lynn G, Mach-Hofacre B, Mueller AJ, Severson GM, Freeman WR. Treatment of herpes retinitis in an animal model with a sustained delivery antiviral drug, Liposomal 1-*O*-octadecyl-*sn*-glycerol-3-phosphonoformate. *Retina* 1999;19:325–331. [PubMed: 10458299]

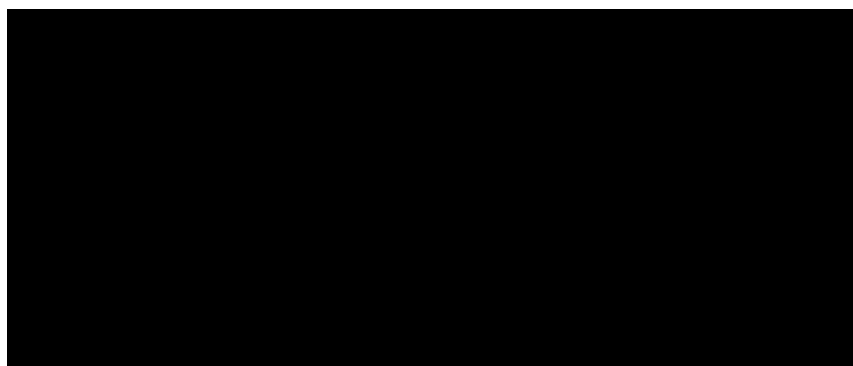


FIGURE 1.
Structure of AG3340.

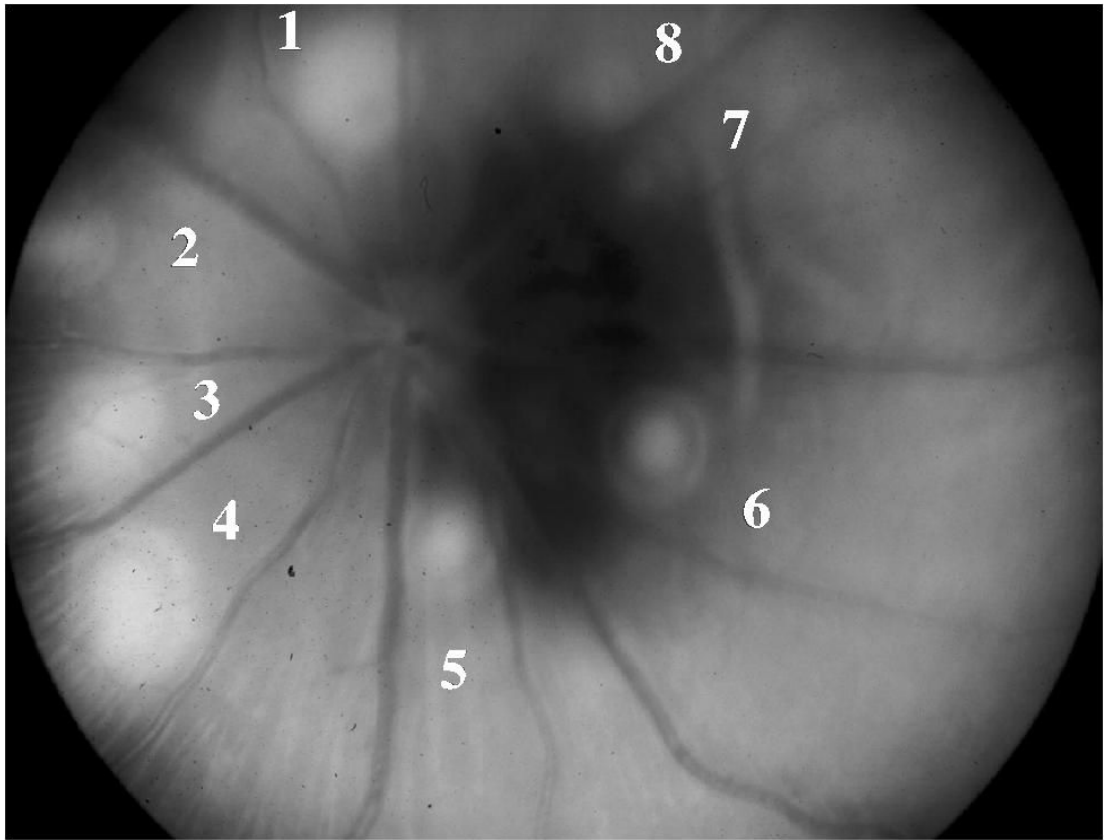


FIGURE 2.
Fundus Photo of One of the Control Eyes of the Pretreatment Group Captured 1 Day After Laser. All eight laser lesions were associated with bubbling.

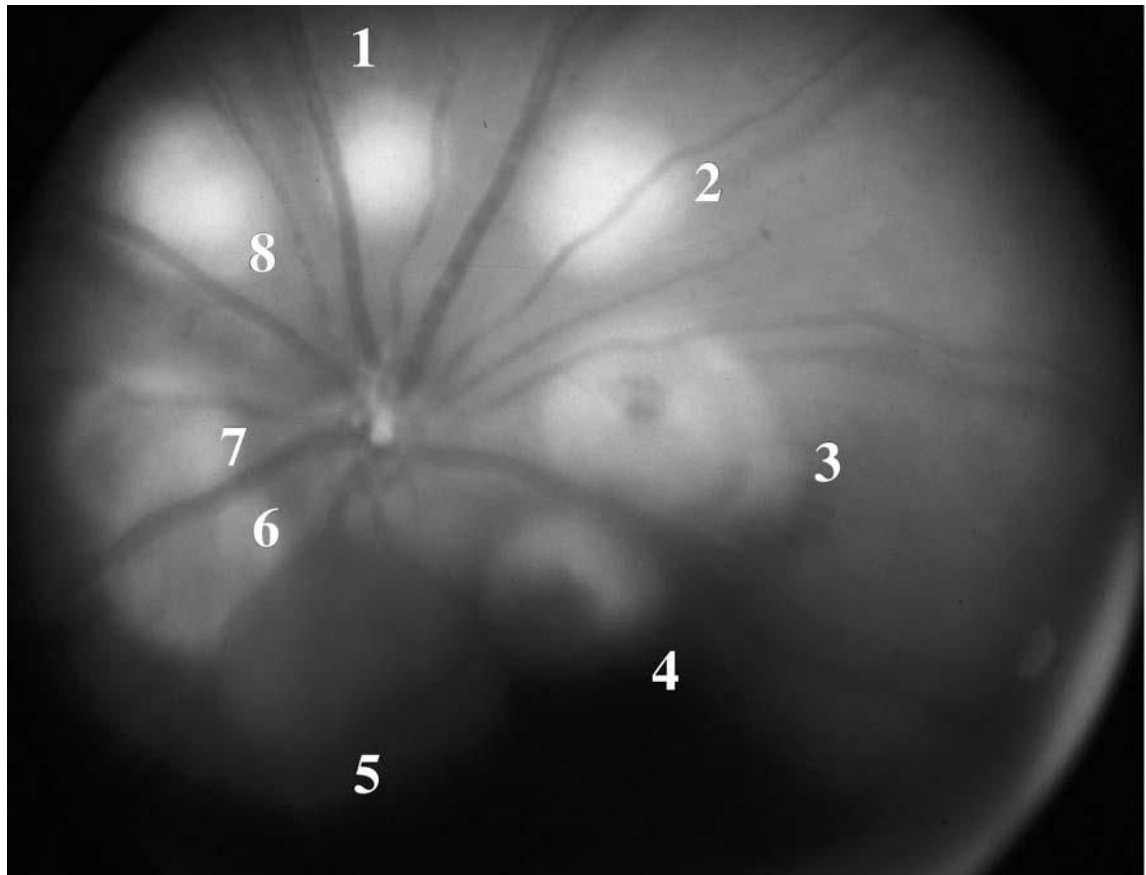


FIGURE 3. Fundus Photo of One of the Treated Eyes of the Pretreatment Group Captured 1 Day After Laser. Lesions 1, 2, and 8 were associated with bubbling. Lesions 6 and 7 were associated with choroidal hemorrhage. Lesions 3 and 4 were associated with retinal hemorrhage. Spot 5 was associated with preretinal hemorrhage.

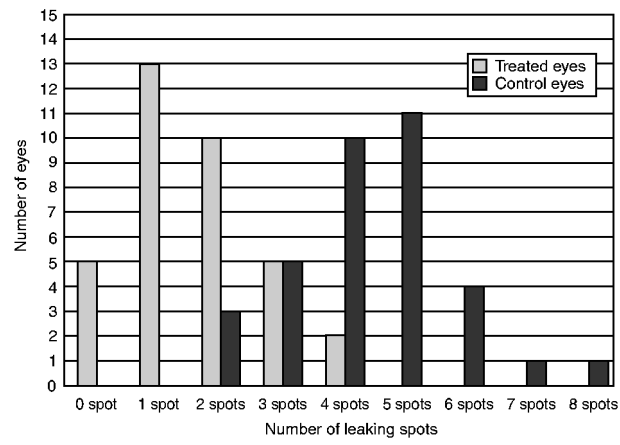


FIGURE 4.
The relationship of the Number of Leaking Spots to the Number of Eyes in Both Groups at 4 Weeks.

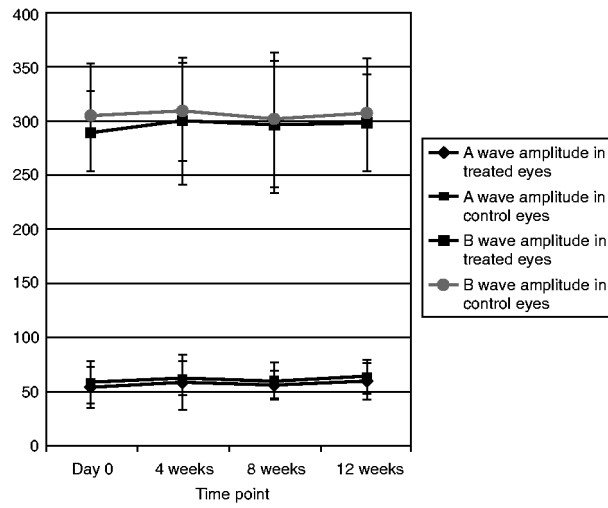


FIGURE 5.
A and B Wave Amplitude Values in Treated and Control Eyes at Different Time Points.

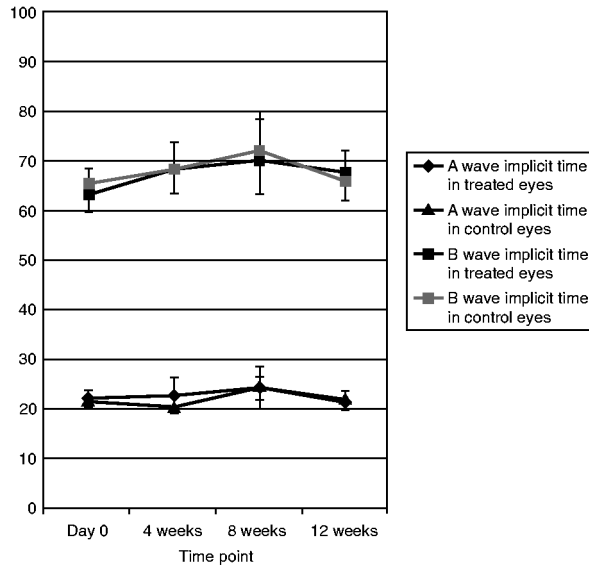


FIGURE 6.
Implicit Time of A and B Waves in Treated and Control Eyes at Different Time Points.



FIGURE 7. Fundus Photo 1 Hour after Drug Injection Showing White Drug Aggregates. The black arrow points to the minimal hemorrhage complicating the drug injection. The two light gray arrows point to the previously done laser lesions.

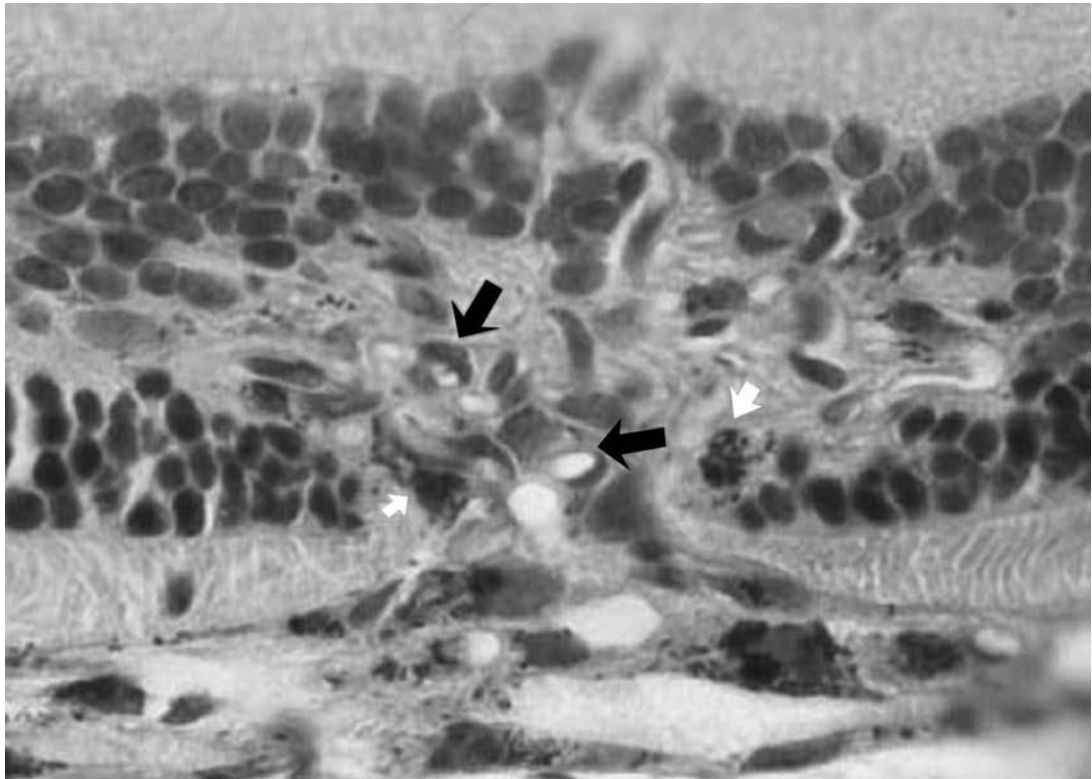


FIGURE 8.
High Magnification (X = 300) of the Previous Section Showing Endothelial Cell Proliferation (Black Arrows) and Pigment-Laden Macrophage Infiltration (White Arrows).

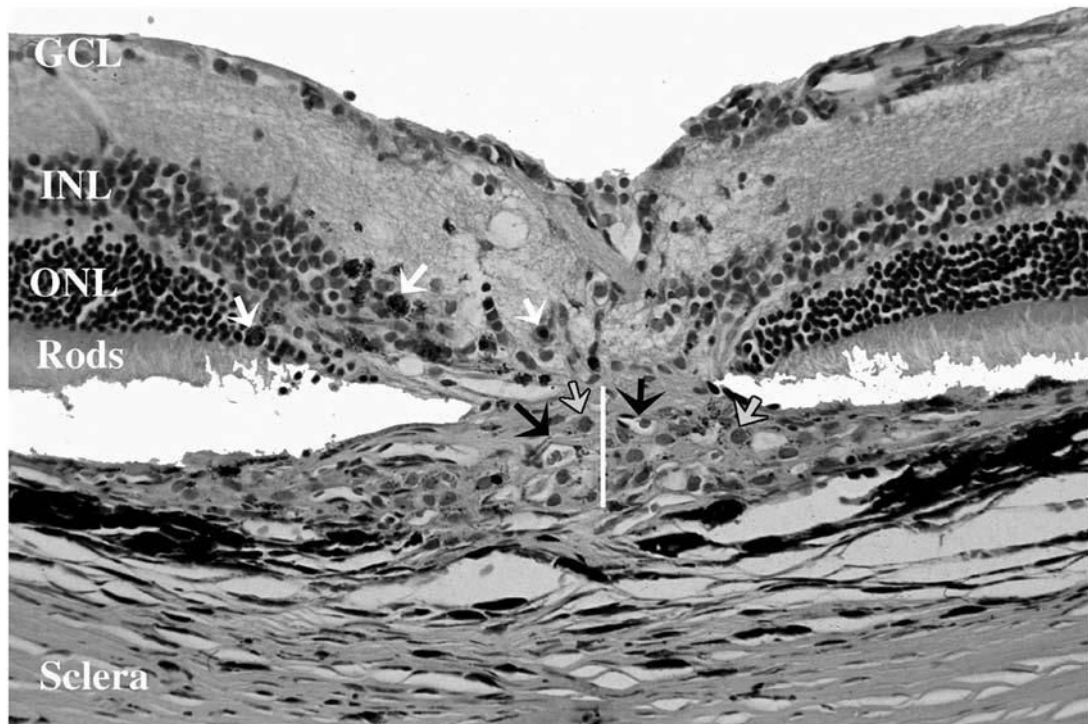


FIGURE 9.

Light Microscopy of a Leaking Laser Spot in a Control Eye 4 Weeks After Laser Showing the Infiltration of the Subretinal Space by Fibrovascular Complex. The thickness of the fibrovascular lesion is demonstrated by the white line. Black arrows point to the proliferating new vessels containing RBCs. Gray arrows point to the infiltrating macrophages while white arrows point to pigment-laden macrophages. Outer and inner segments of photoreceptors, outer nuclear layer (ONL), and inner nuclear layer (INL) are disrupted by the laser. (H & E stain, original magnification X = 130).

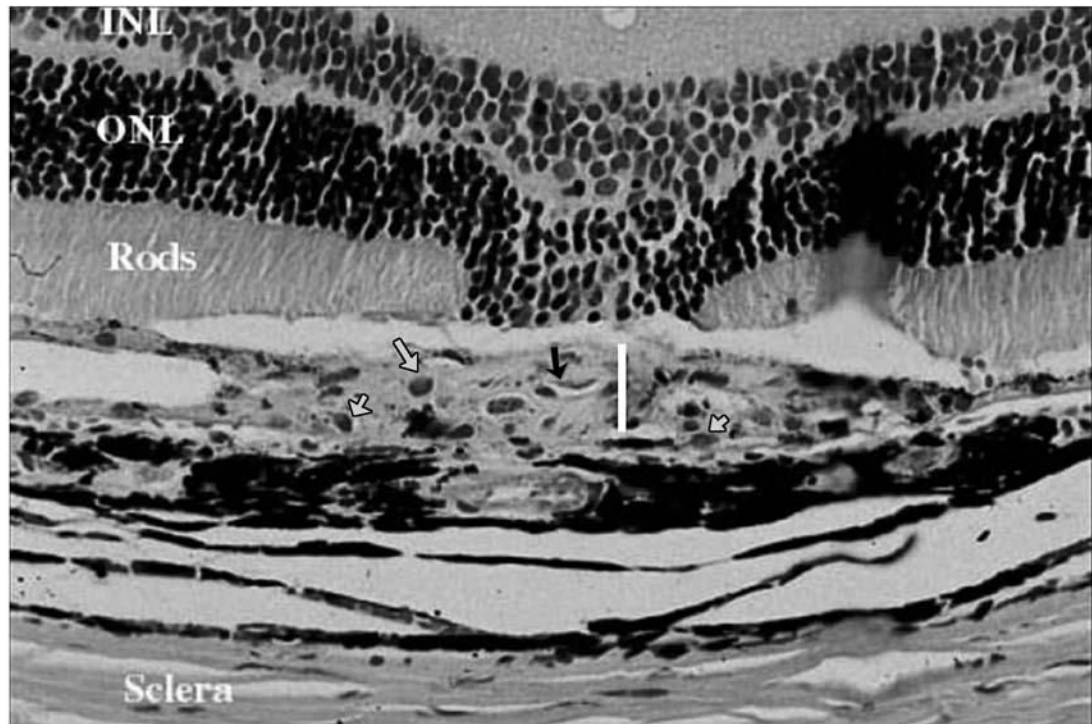


FIGURE 10.

Light Microscopy of a Leaking Laser Spot in a Treated Eye 4 Weeks After Laser Showing a Thinner Fibrovascular Complex (White Line) Compared to Controls. The proliferating new blood vessels are also less dense and lack RBCs inside their lumen (black arrow). The density of infiltrating macrophages (gray arrows) is the same as in control eyes. (H & E stain, original magnification X = 130).

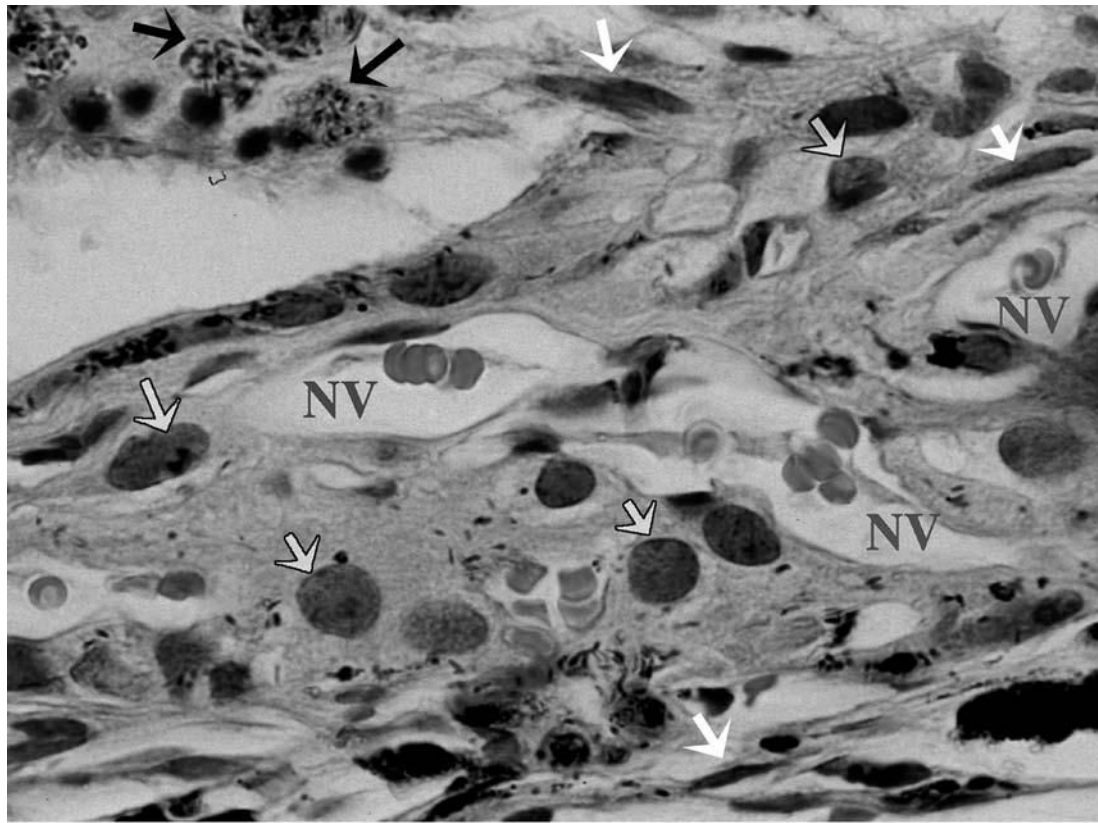


FIGURE 11. High Magnification Showing the Structure of Induced Choroidal Neovascular Membrane in One of the Control Eyes 4 Weeks After Laser Consisting of Proliferating Endothelial Cells Forming New Vessels (NV) Containing RBCs, Spindle-Shaped Cells (fibroblasts) Pointed to by White Arrows, Macrophages (Gray Arrows), and Pigment Laden Cells (Black Arrows). (H & E stain, original magnification X = 330).

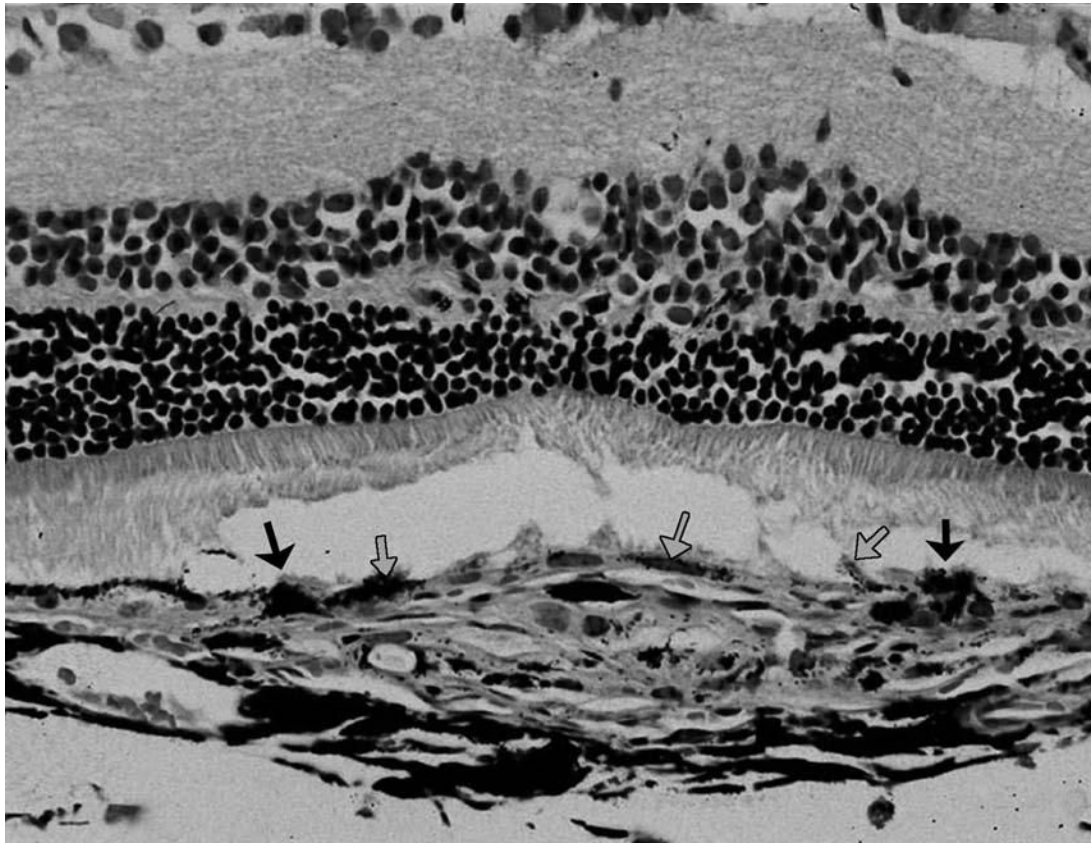


FIGURE 12.

Light Micrograph of One of the Control Eyes 8 Weeks After Laser Showing the Healing Pattern of RPE Cells. The RPE cells at the edge of the laser burn (black arrows) show marked thickening and proliferation in more than one layer. The gray arrows point to the proliferating RPE cells over the fibrovascular complex. (H & E stain, original magnification X = 130).

Table 1

Baseline Characteristics of the Laser Lesions in Both Treated and Control Groups of the Pretreatment Group

Group	Bubbling	Bubbling plus choroidal hemorrhage	Bubbling plus choroidal & retinal hemorrhage	Bubbling plus preretinal hemorrhage	Total
Treated eyes	115/280 (41%)	46/280 (16.4%)	71/280 (25.4%)	48/280 (17.2%)	280/280 (100%)
Control eyes	115/280 (41%)	62/280 (22.1%)	60/280 (21.4%)	43/280 (15.5%)	280/280 (100%)
<i>p</i> Value	1.00	0.11	0.32	0.32	

The data in the table were compared using Fisher's exact test.

All the compared data in this table were statistically insignificant ($p > 0.05$).

The total 280 in the table represents the total number of laser lesions in all eyes in each group (35 eyes multiplied by 8 laser lesions per each eye).

Table 2

Percentage of Leaking Laser Lesions in Treated and Control Eyes as Evaluated by Fluorescein Angiography at Different Time Points

Time point	Treated eyes				Control eyes			
	Nonleaking	Leaking	N/A	Total	Nonleaking	Leaking	N/A	Total
2 weeks	195/246 (79.3%)	51/246 (20.7%)	34	280	106/243 (43.6%)	137/243 (56.4%)	37	280
4 weeks	190/246 (77.2%)	56/246 (22.8%)	34	280	93/250 (37.2%)	157/250 (62.8%)	30	280
8 weeks	106/127 (83.5%)	21/127 (16.5%)	17	144	52/130 (40%)	78/130 (60%)	14	144
12 weeks	61/71 (85.9%)	10/71 (14.1%)	1	72	29/70 (41.4%)	41/70 (58.6%)	2	72

p value was statistically significant as regard the comparison of the percentage of leakage in both groups at all time points ($p < 0.0001$). The data in the table were compared using Fisher's exact test.

N/A, not applicable.

Table 3

Association of Hemorrhage with Percentage of Leakage in Control Eyes at 4-Week Time Point

Laser spot condition	Leaking lesions	Nonleaking lesions	N/A	Total
Bubbling	49/114 (43%)	65/114 (57%)	1	115
Bubbling and hemorrhage	108/136 (79.4%)	28/136 (20.6%)	29	165

$p < 0.0001$ (Fisher's exact test).

N/A (nonapplicable) due to masking by overlying blood.

115 represents the total number of laser lesions associated with bubbling at the time of laser application while 165 represents the total number of laser lesions that were associated with various types of hemorrhage at the time of laser application.

Table 4
Percentage of Leakage in Both Treated and Control Eyes in the Posttreatment Group

Time point	Treated eyes			Control eyes			p value*
	Leaking	Nonleaking	N/A	Leaking	Nonleaking	N/A	
2 weeks	104/197 (52.2%)	93/197 (47.2%)	3	96/191 (50.3%)	95/191 (49.7%)	9	0.685
4 weeks	107/198 (54.1%)	91/198 (45.9%)	2	115/195 (58.9%)	80/195 (41.1%)	5	0.361
8 weeks	51/104 (49%)	53/104 (51%)	0	56/101 (55.4%)	45/101 (44.6%)	3	0.402
12 weeks	24/48 (50%)	24/48 (50%)	0	25/46 (54.4%)	21/46 (45.6%)	2	0.685

N/A, not applicable.

* p value was evaluated using Chi-square